ACS OMEGA

http://pubs.acs.org/journal/acsodf

Article

Intermolecular Copigmentation of Malvidin-3-*O*-glucoside with Caffeine in Water: The Effect of the Copigment on the pH-Dependent Reversible and Irreversible Processes

Ambrósio Camuenho, André Seco, A. Jorge Parola, Nuno Basílio, and Fernando Pina*

Cite This: *ACS Omega* 2022, 7, 25502−25509

Read Online

ACCESS | Metrics & More | Article Recommendations

ABSTRACT: Intermolecular copigmentation of malvidin-3-*O*-glucoside with caffeine was studied using a holistic procedure that includes the extension to basic pH values. In moderately basic solutions (7.5 < pH < 9.5) and independently of the copigment presence, there is a pH region where degradation of the quinoidal base and anionic quinoidal bases is faster than hydration and OH^- nucleophilic addition, preventing the system from reaching the equilibrium. Intermolecular copigmentation with caffeine reduces significantly the degradation rate of quinoidal bases. In a more basic medium, the equilibrium is reached and degradation occurs from the anionic chalcones. In this case, the addition of caffeine also reduces the degradation rate in the interval 10 < pH < 11.5.

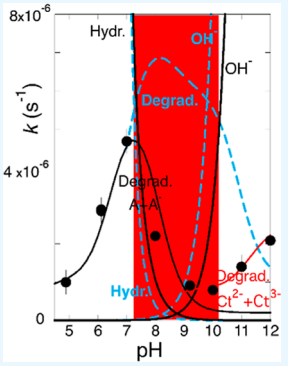

1. INTRODUCTION

Anthocyanins are ubiquitous molecules that confer color to the majority of angiosperms.[1] By presenting an attractive color, they favor plant reproduction, attracting pollinators and seed dispersers,[2,3] protect plants from several biotic and abiotic stresses,[4,5] and function as photoprotective agents by absorbing excess visible and UV light.[6,7] The consumption of anthocyanin-rich foods has been associated with numerous beneficial health effects due to their biological properties such as antiproliferative, anti-inflammatory, and antimicrobial properties.[8−12] However, anthocyanins have a severe drawback. They are not stable enough for most of the applications that imply relatively long storage periods.[13−16] Intermolecular copigmentation is used by plants to extend the pH domain of the red flavylium cation and increase the purple color of the quinoidal base.[14] The question is as follows: did intermolecular copigmentation also have some protecting effect on the anthocyanin's degradation? From this perspective, the tools of the physical chemistry, in particular the studies concerning the pH-dependent thermodynamics and kinetics of anthocyanins, are indispensable to characterize both reversible and irreversible processes occurring in these compounds.[14] This knowledge is critical to design protection strategies to stabilize anthocyanins.

1.1. Reversible versus Irreversible Reactions in Anthocyanins. *1.1.1. Reversible Equilibrium. 1.1.1.1. Direct pH Jumps.* The reversible sequence of chemical reactions that follow the addition of the base to equilibrated solutions of the flavylium cation of malvidin-3-*O*-glucoside at pH ≤ 1 (direct pH jumps) is illustrated in Scheme 1.[14,17,18] The first reaction consists of flavylium cation deprotonation to give the respective quinoidal bases with a mole fraction distribution dependent on the final pH. These deprotonation processes are very fast and occur during the mixing time of the stopped flow (first step).[19] Nevertheless, it is possible to calculate the respective acid−base constants (first column of Scheme 1) by collecting the absorption spectra using a stopped flow 10 ms after the mixture of the base and representing the absorption versus pH plot at representative wavelengths, as reported in Figure 3a.

The quinoidal bases are kinetic products that disappear through the hydration reaction, followed by a faster tautomerization (second step). In the second step, $\mathbf{AH}^+$ and all quinoidal bases (their mole fraction distribution depending on the pH) are in fast equilibrium on one side and **B** and **Cc** and the respective anionic forms on the other side. One breakthrough fundamental for the understanding of the multi-equilibria was reported by Brouillard and Dubois,[17] who showed that quinoidal bases do not hydrate and the systems move toward the equilibrium due to the hydration of the

Received: April 25, 2022
Accepted: June 16, 2022
Published: July 12, 2022

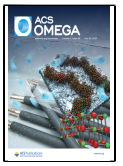

Scheme 1. Sequence of Reversible Reactions upon the Addition of the Base to Equilibrated Solutions of the Flavylium Cation of Malvidin-3-*O*-glucoside at pH ≤ 1 (Direct pH Jumps)[a]

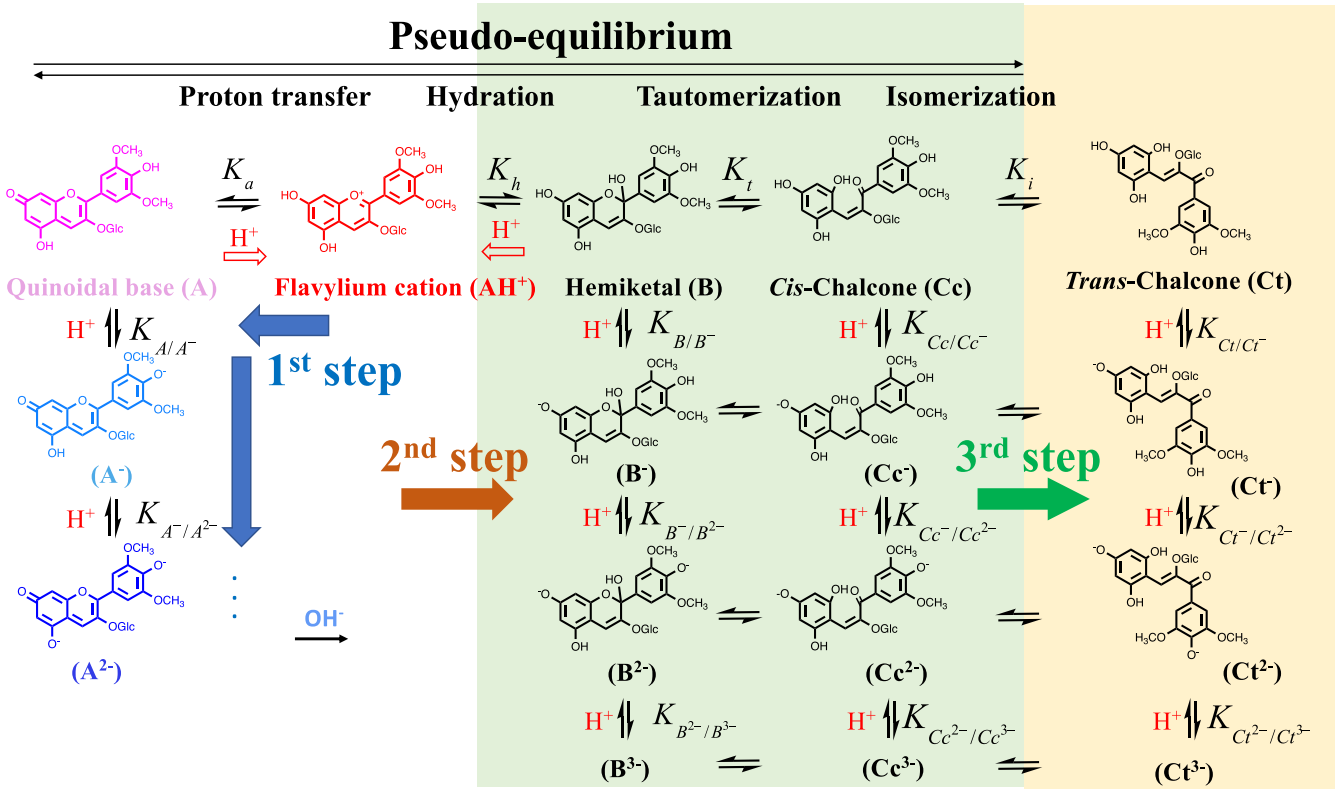

[a]This scheme is followed by all anthocyanins. Adapted with permission from ref 19. Copyright 2022. American Chemical Society.

flavylium cation. The kinetics of the second step is given by eq 1, where χ_{AH+} corresponds to the mole fraction of $\mathbf{AH^+}$ in its equilibrium with **A** and $\mathbf{A^-}$ and χ_B corresponds to the mole fraction of **B** in its equilibrium with $\mathbf{B^-}$, **Cc**, and $\mathbf{Cc^-}$.

$$k_{2nd} = \chi_{AH^+}k_h + \chi_B k_{-h}[H^+] = \frac{[H^+]^2}{[H^+]^2 + K_a[H^+] + K_aK_{A/A^-}}k_h + \frac{[H^+]}{(1+K_t)[H^+] + K_{B/B^-} + K_{Cc/Cc^-}K_t}k_{-h}[H^+] + k_{OH}[OH^-] \quad (1)$$

In eq 1, the reaction channel occurring in the basic medium due to the OH^- nucleophilic addition was added.[14] When the formation of the anionic species was not considered, the experimental data is accounted for by eq 2.

$$k_{2nd} = \chi_{AH^+}k_h + \chi_B k_{-h}[H^+] = \frac{[H^+]}{[H^+] + K_a}k_h + \frac{1}{(1+K_t)}k_{-h}[H^+] \quad (2)$$

Inspection of eq 1 shows that the rate of the second step tends to zero with the increase in pH and the rate of OH^- nucleophilic addition also tends to zero with the increase in pOH. This is a very relevant result crucial for the rationalization of anthocyanin degradation, see below.

The system reaches the equilibrium through the much slower cis−trans isomerization. In this case, all species except *trans*-chalcones are in equilibrium, defining the pseudo-equilibrium (identified by the superscript ˆ). During isomerization, the flavylium cation and all quinoidal bases, hemiketals, and *cis*-chalcones are in faster equilibrium, allowing for the deduction of the respective observed rate constant, eq 3.

$$k_{3rd} = \chi_{Cc}k_i + \chi_{Ct}k_{-i} + \chi_{Cc^-}k_{i^-} + \chi_{Ct^-}k_{-i^-} \quad (3)$$

In eq 3, k_i and k_{-i} are the direct and reverse rate constants for the formation of **Ct** from **Cc**, respectively, χ_{Cc} is the mole fraction of **Cc** at the pseudo-equilibrium, and χ_{Ct} is the mole fractions of **Ct** in its equilibrium with $\mathbf{Ct^-}$, *mutatis mutandis*, for the isomerization of $\mathbf{Cc^-}/\mathbf{Ct^-}$.

The equilibrium of the first row of Scheme 1 is accounted for by eqs 4−7

$$\mathbf{AH^+} + H_2O \underset{k_{-a}}{\overset{k_a}{\rightleftharpoons}} \mathbf{A} + H_3O^+ \; K_a \text{ proton transfer} \quad (4)$$

$$\mathbf{AH^+} + 2H_2O \underset{k_{-h}}{\overset{k_h}{\rightleftharpoons}} \mathbf{B} + H_3O^+ \; K_h \text{ hydration} \quad (5)$$

$$\mathbf{B} \underset{k_{-t}}{\overset{k_t}{\rightleftharpoons}} \mathbf{Cc} \; K_t \text{ tautomerization} \quad (6)$$

https://doi.org/10.1021/acsomega.2c02571
ACS Omega 2022, 7, 25502−25509

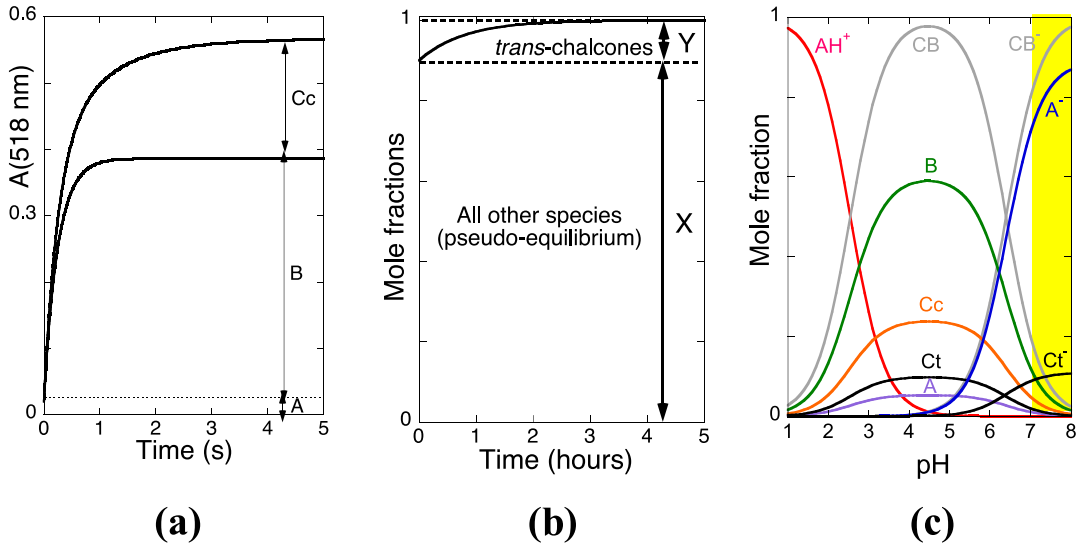

Figure 1. (a) Trace of the reverse pH jump of malvidin-3-*O*-glucoside at pH = 5.5; (b) trace of malvidin-3-*O*-glucoside obtained using a common spectrophotometer; and (c) mole fraction distribution of the malvidin-3-*O*-glucoside species at the equilibrium. The yellow band corresponds to the region where equilibrium is not attained. Adapted with permission from ref 21. Copyright 219. American Chemical Society.

$$\mathbf{Cc} \underset{k_{-i}}{\overset{k_i}{\rightleftharpoons}} \mathbf{Ct}\ K_i \text{ isomerization} \tag{7}$$

This multi-equilibrium can be simplified considering a single acid−base system, eq 8

$$\mathbf{AH}^+ + H_2O \rightleftharpoons \mathbf{CB} + H_3O^+\ K_a' = \frac{[CB][H^+]}{[AH^+]} \text{ global equilibrium} \tag{8}$$

with $K_a' = K_a + K_h + K_hK_t + K_hK_tK_i$ and

$$[CB] = [A] + [B] + [Cc] + [Ct] \tag{9}$$

According to eq 8, the complex multi-equilibrium given by eqs 4−7 is equivalent to the single acid−base equilibrium between the flavylium cation and its conjugated base CB, equal to the sum of A, B, Cc, and Ct, given in eq 9.

Extending to the neutral species, eqs 10−14are obtained

$$\mathbf{A} + H_2O \rightleftharpoons \mathbf{A}^- + H_3O^+\ K_{A/A^-} \tag{10}$$

$$\mathbf{B} + H_2O \rightleftharpoons \mathbf{B}^- + H_3O^+\ K_{B/B^-} \tag{11}$$

$$\mathbf{Cc} + H_2O \rightleftharpoons \mathbf{Cc}^- + H_3O^+\ K_{Cc/Cc^-} \tag{12}$$

$$\mathbf{Ct} + H_2O \rightleftharpoons \mathbf{Ct}^- + H_3O^+\ K_{Ct/Ct^-} \tag{13}$$

A similar simplification can be done to obtain eq 14

$$\mathbf{CB} + H_2O \rightleftharpoons \mathbf{CB}^- + H_3O^+\ K_a'' \text{ global equilibrium} \tag{14}$$

with K''_a given by eq 15

$$K_a'' = \frac{[CB^-][H^+]}{[CB]} = \frac{K_{A/A^-}K_a + K_{B/B^-}K_h + K_{Cc/Cc^-}K_hK_i + K_{Ct/Ct^-}K_hK_tK_i}{K_a'} \tag{15}$$

and $[CB^-] = [A^-] + [B^-] + [Cc^-] + [Ct^-]$

In general, in acid to slightly basic solutions, the complex multi-equilibrium of anthocyanins can be reduced to a diprotic acid with constants K'_a and K''_a.

Considering that the isomerization reaction is by far the slowest kinetic step of the system, a pseudo-equilibrium is attained when the observation time falls in the time range of seconds to a few minutes as in the stopped flow measurements.

$$\mathbf{AH}^+ + H_2O \rightleftharpoons \mathbf{CB}\hat{} + H_3O^+K_a\hat{} = \frac{[CB\hat{}][H^+]}{[AH^+]} \text{ global equilibrium} \tag{16}$$

$$\text{with } K_a\hat{} = K_a + K_h + K_hK_t \text{ and } [CB\hat{}] = [A] + [B] + [Cc] \tag{17}$$

$$CB\hat{} + H_2O \rightleftharpoons CB\hat{}^- + H_3O^+\ K_a\hat{\hat{}} \text{ global equilibrium} \tag{18}$$

$$K_a\hat{\hat{}} = \frac{[CB\hat{}^-][H^+]}{[CB]} = \frac{K_{A/A^-}K_a + K_{B/B^-}K_h + K_{Cc/Cc^-}K_hK_i}{K_a\hat{}}$$

$$\text{and } [CB^-] = [A^-] + [B^-] + [Cc^-] + [Ct^-] \tag{19}$$

In conclusion, in acid medium up to neutral-slightly basic, the equilibrium and the pseudo-equilibrium are equivalent to a diprotic acid and the mole fraction distribution of $\mathbf{AH}^+$, **CB**, and $\mathbf{CB}^-$ or the equivalent species, at the pseudo-equilibrium substituting K'_a and K''_a by K_a and K_a, are given by eq 20.

$$\chi_{AH^+} = \frac{[H^+]^2}{[H^+]^2 + K_a'[H^+] + K_a'K_a''};\quad \chi_{CB} = \frac{K_a'[H^+]}{[H^+]^2 + K_a'[H^+] + K_a'K_a''};\quad \chi_{CB^-} = \frac{K_a'K_a''}{[H^+]^2 + K_a'[H^+] + K_a'K_a''} \tag{20}$$

1.1.1.2. Reverse pH Jumps. Reverse pH jumps consist in the addition of the acid, generally back to the flavylium cation at pH ≤ 1, to equilibrated solutions or pseudo-equilibrated solutions at higher pH values.[20−22] As shown above in eq 1, the rate of the hydration reaction increases with the increasing proton concentration. At sufficiently acidic solutions (namely, at pH ≤ 1), the hydration reaction becomes faster than

https://doi.org/10.1021/acsomega.2c02571
ACS Omega 2022, 7, 25502−25509

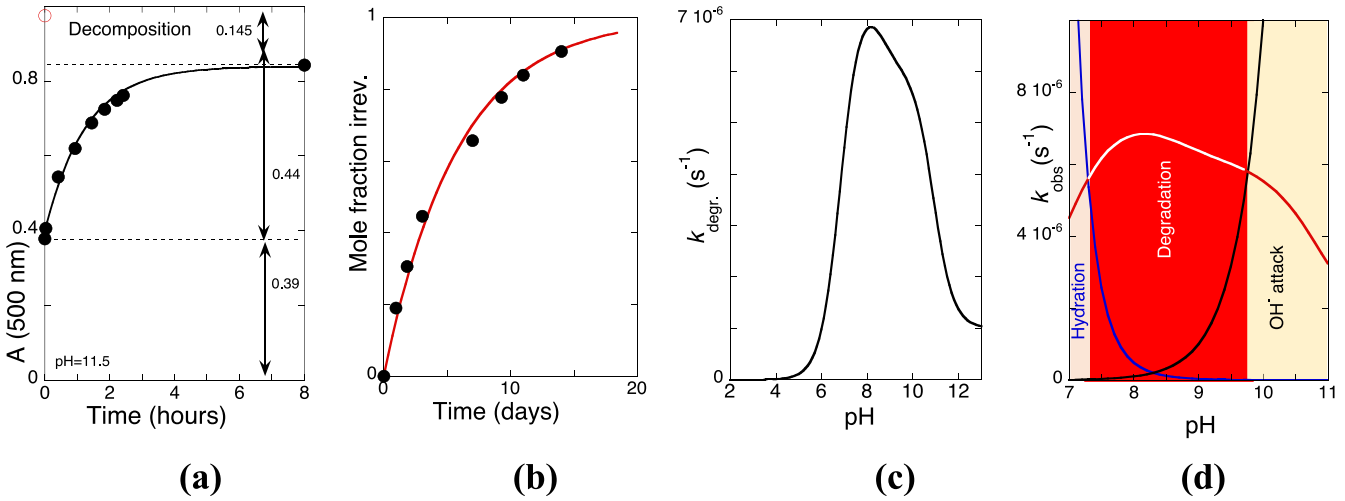

Figure 2. (a). Recovery of the malvidin-3-*O*-glucoside flavylium cation after 1 day of delay time, at pH = 11.6, with the red open circle representing the initial flavylium cation absorption; (b) decomposition mole fraction as a function of time, at pH = 11.6, calculated using eq 26, behaves as a mono-exponential from which the degradation rate constant can be calculated; (c) degradation rate of malvidin-3-*O*-glucoside as a function of pH; and (d) comparison between the reversible reactions, hydration and OH^- nucleophilic addition, and the degradation rate. Adapted with permission from ref 19. Copyright 2022. American Chemical Society.

tautomerization, the so-called change of regime.[14,20] The reverse pH jumps rates involving all species except *trans*-chalcones fall in the domain of seconds, requiring a stopped flow apparatus, while for the *trans*-chalcones, they occur in hours and can be monitored using a common spectrophotometer. In other words, during stopped flow measurements, the *trans*-chalcone is "frozen". In Figure 1,the trace of a reverse pH jump of malvidin-3-*O*-glucoside from pH = 5.5 monitored by stopped flow is shown. Three amplitudes can be observed (Figure 1a). The first corresponds to the remaining flavylium cation and quinoidal bases that are converted in the flavylium cation during the mixing time of the stopped flow (at pH = 5.5, mainly A). The amplitude of the faster kinetic process corresponds to the conversion of hemiketal in the flavylium cation, and the amplitude of the slower kinetics is the conversion of *cis*-chalcone in more flavylium cations via hemiketal.[14,20] Normalization of the amplitudes of Figure 1a gives the respective mole fractions. Fitting of the mole fractions of the pseudo-equilibrium species as a function of pH (see below, Figure 3c) can be achieved by means of eq 21a.

$$\chi_{AH^+} + \chi_A + \chi_{A^-} = \frac{[H^+]^2 + a_0\hat{K_a}[H^+] + a_1\hat{K_a}\hat{\hat{K_a}}}{[H^+]^2 + \hat{K_a}[H^+] + \hat{K_a}\hat{\hat{K_a}}} \quad (21a)$$

$$\chi_B + \chi_{B^-} = \frac{[H^+]^2 + b_0\hat{K_a}[H^+] + b_1\hat{K_a}\hat{\hat{K_a}}}{[H^+]^2 + \hat{K_a}[H^+] + \hat{K_a}\hat{\hat{K_a}}} \quad (21b)$$

$$\chi_{Cc} + \chi_{Cc^-} = \frac{[H^+]^2 + c_0\hat{K_a}[H^+] + c_1\hat{K_a}\hat{\hat{K_a}}}{[H^+]^2 + \hat{K_a}[H^+] + \hat{K_a}\hat{\hat{K_a}}} \quad (21c)$$

with $a_0 + b_0 + c_0 = a_1 + b_1 + c_1 = 1$.

Once the coefficients a, b, and c are obtained, the equilibrium constants of the respective species are straightforwardly calculated from the relations of eqs 22 and 23.[21]

For the neutral species

$$K_a = a_0\hat{K_a};\ K_h = b_0\hat{K_a};\ K_hK_t = c_0\hat{K_a} \quad (22)$$

Additionally, for the anionic species

$$K_{A/A^-} = \frac{a_1\hat{K_a}\hat{\hat{K_a}}}{K_a};\ K_{B/B^-} = \frac{b_1\hat{K_a}\hat{\hat{K_a}}}{K_h};\ K_{Cc/Cc^-} = \frac{c_1\hat{K_a}\hat{\hat{K_a}}}{K_hK_t} \quad (23)$$

The isomerization rate constants are calculated by means of a reverse pH jump from the equilibrium carried out using a common spectrophotometer (see Figure 1b). The amplitude of the flavylium at the initial time corresponds to the sum of $\mathbf{AH^+} + \mathbf{A} + \mathbf{B} + \mathbf{Cc}$ and the amplitude of the very slow process (i.e., controlled by the isomerization) permits the calculation of parameters d_0 and d_1 using eq 24 and consequently K_i and $K_{Ct/Ct-}$ using eq 25. Having obtained all equilibrium constants, the pH-dependent mole fraction distribution of the species at the equilibrium is straightforwardly obtained, as shown in Figure 1c.[14]

$$\chi_{Ct} + \chi_{Ct^-} = \frac{d_0K_a'[H] + d_1K_a'K_a''}{[H^+]^2 + K_a'[H] + K_a'K_a''} \quad (24)$$

$$K_i = \frac{d_0K_a'}{K_hK_t};\ K_{Ct/Ct^-} = \frac{d_1K_a'K_a''}{K_hK_tK_i} \quad (25)$$

1.1.2. Irreversible Equilibrium. Recently, we reported on an experimental procedure to account for the calculation of the degradation rate in anthocyanins.[19] It is based on a sequence of pH jumps as follows: (i) direct pH jump to an extended pH region including the basic medium; (ii) maintaining the solution at the final pH of the direct pH jump; (iii) taking one aliquot of (ii) after 1 day and performing a reverse pH jump back to pH ≤ 1; and (iv) repeating (iii) for different delay times and calculating the disappearance of the flavylium cation as a function of time. The degradation fraction for each pH value, $\chi_{decomposition}$, is calculated using eq 26.

$$\chi_{decomposition} = 1 - \chi_{AH^+recovery} = 1 - \frac{A_{after\ delay}}{A_{initial}} \quad (26)$$

A typical result of the flavylium recovery after a certain delay time is shown in Figure 2a. It is possible to calculate the fraction of the flavylium cation that disappeared for each delay time and obtain the degradation rate for each pH value, as

https://doi.org/10.1021/acsomega.2c02571
ACS Omega 2022, 7, 25502−25509

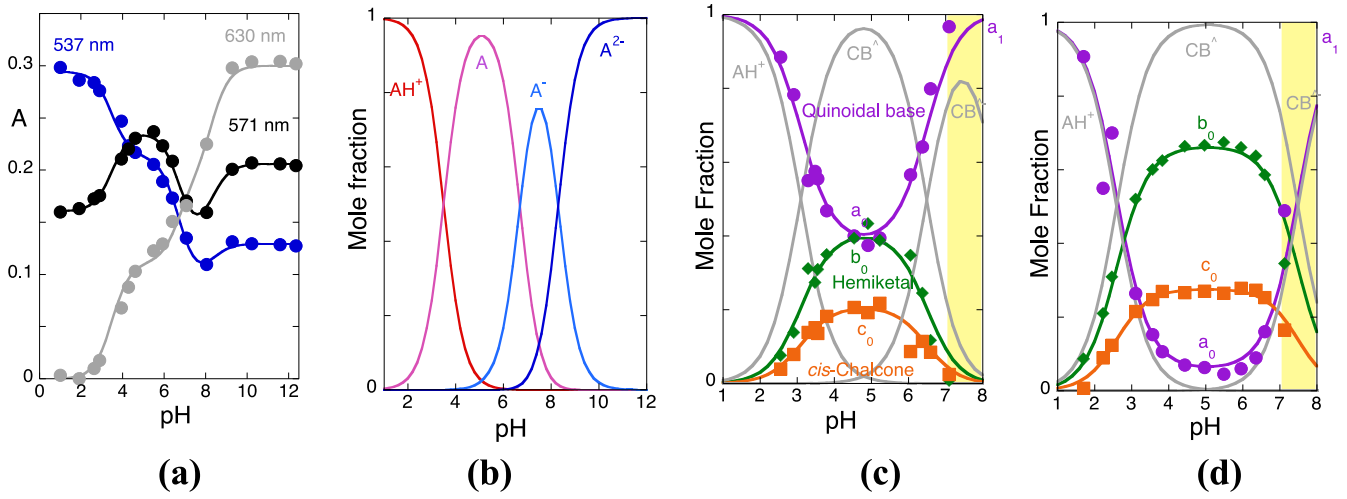

Figure 3. (a) Titration curves of malvidin-3-*O*-glucoside in the presence of caffeine 0.05 M collected by stopped flow 10 ms after a direct pH jump from the flavylium cation at pH = 1 at three representative wavelengths. Fitting was achieved for pK_a = 3.5, $pK_{A/A-}$ = 6.7, and $pK_{A-/A2-}$ = 8.3; (b) mole fraction distribution of the malvidin-3-*O*-glucoside species, flavylium cation, and quinoidal bases in the presence of caffeine taken 10 ms after a direct pH jump; and (c) mole fraction distribution of malvidin-3-*O*-glucoside in the presence of caffeine at the pseudo-equilibrium after a series of pH jumps monitored by stopped flow and (d) in the absence of caffeine for comparison purposes. Figure 3c,d, Reprinted with permission from ref 21. Copyright 2019. American Chemical Society.

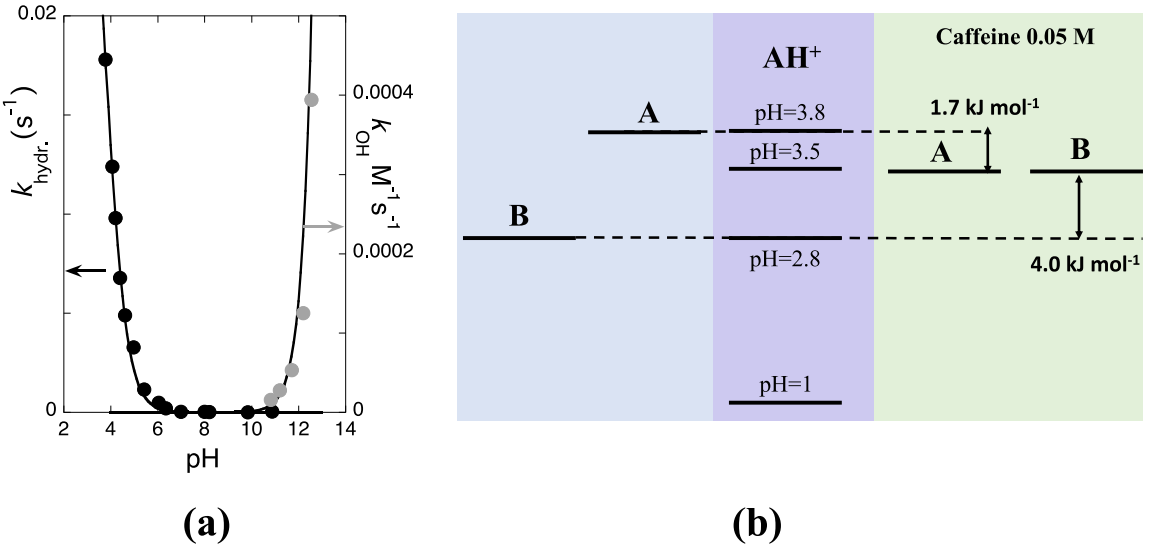

Figure 4. (a) Hydration reaction of malvidin-3-*O*-glucoside in the presence of caffeine 0.05 M. Fitting was achieved by means of eq 27 for k_h = 0.045 s^{-1}, k_{-h} = 150 $M^{-1}s^{-1}$, and the values of the protonation constants reported in Figure 3a; (b) relative energy level of B and A in the absence and presence of caffeine.

shown in Figure 2b. Finally, the degradation rate as a function of pH, given in Figure 2c, can be calculated. The comparison between the reversible processes (hydration and OH^- nucleophilic addition) and the degradation rate allows for the detection of a pH range where the equilibrium is not attained. In fact, as shown in Figure 2d, in the pH region highlighted in red, degradation is faster than any other process toward the equilibrium. The rationalization of the anthocyanin degradation implies the determination of this pH interval.

The question is how to quantify the effect of intermolecular copigmentation[23−25] in anthocyanin degradation. In this work, the copigmentation between malvidin-3-*O*-glucoside and caffeine was used to illustrate this phenomenon. In particular, caffeine was selected to avoid cinnamic acids, the most common copigments, which have two forms at the working pH range, neutral and negatively charged, interacting differently with the several anthocyanin species, as shown in Scheme 1.[26] These copigments would introduce an additional level of complexity that would compromise the clarity of the exposition.[27]

2. RESULTS AND DISCUSSION

2.1. Reversible Processes. In Figure 3, the titration of the quinoidal bases of malvidin-3-*O*-glucoside in the presence of caffeine 0.05 M was monitored by stopped flow 10 ms after a direct pH jump is reported. Fitting was achieved for pK_a = 3.5, $pK_{A/A-}$ = 6.7, and $pK_{A-/A2-}$ = 8.3. This allows for calculating the mole fraction distribution of the quinoidal species (first column of Scheme 1) in the presence of the copigment, as shown in Figure 3b. When the acid base constants in the absence of caffeine, pK_a = 3.8, $pK_{A/A-}$ = 6.3, and $pK_{A-/A2-}$ = 8.4, are compared with those in its presence, there is an evident

https://doi.org/10.1021/acsomega.2c02571
ACS Omega 2022, 7, 25502−25509

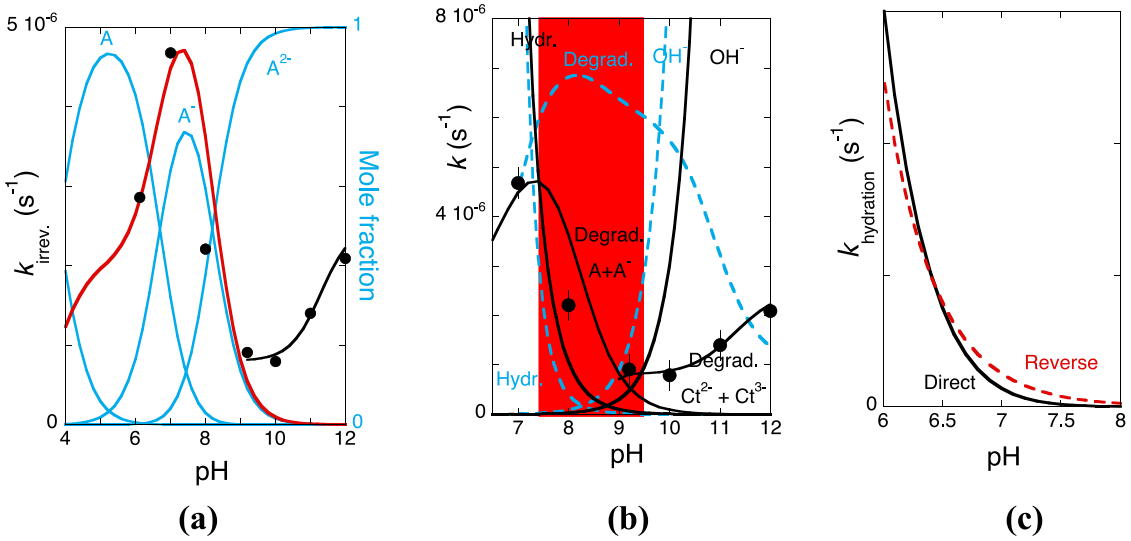

Figure 5. (a) Rate constants of the irreversible processes of malvidin-3-*O*-glucoside in the presence of caffeine 0.05 M. (b) Representation of the hydration, OH^- nucleophilic addition, and degradation rates of malvidin-3-*O*-glucoside in the absence (blue traced lines) and in the presence of caffeine 0.05 M (black full lines), eq 28 (red band) and eq 29 (higher pH values); the red band corresponds to the pH region where the equilibrium is not attained. (c) Contribution for the hydration reaction rate of the term dependent on k_h (direct) and the term depending on k_{-h} (reverse) in eq 27.

decrease of pK_a in the presence of caffeine. This indicates that the quinoidal base is more stabilized than the flavylium cation by caffeine and its pH domain is also extended to higher pH values. This result contrasts with the interaction of malvidin-3-*O*-glucoside with lignosulfonate, where pK_a increases to 4.4 due to the stabilization of the flavylium cation by the negatively charged lignosulfonate.[28]

The stabilization of the quinoidal base by the caffeine is evident in the comparison of Figure 3c with Figure 3d, where the mole fraction distribution of the species at the pseudo-equilibrium in the absence of caffeine is reported. It is worth noting that in the reverse pH jump experiments shown in Figure 3c,d, the parameters are as follows: $a_1 = 1$ and $b_1 = c_1 = 0$. This was an unexpected result because it suggests that near the neutrality, the only observed species is the quinoidal base. The reason, discussed below in detail, is that in a pH region between neutral and slightly basic, the irreversible processes involving quinoidal bases are the rate-determining step of their relatively slow disappearance.

The pH-dependent rate constants of the second kinetic step (controlled by the hydration reaction in the acidic medium and OH^- nucleophilic addition in the basic medium) of malvidin-3-*O*-glucoside in the presence of caffeine 0.05 M as a function of pH are shown in Figure 4a.

Considering that the formation of B^- and Cc^- does not take place since they fall in the pH range where the degradation reactions of A^- and A^{2-} are the rate-determining steps (see below), eq 1 is simplified to eq 27, and fitting was achieved for $k_h = 0.045\ s^{-1}$, $k_{-h} = 150\ M^{-1}s^{-1}$, $k_{OH} = 0.03\ M^{-1}s^{-1}$, and the values of the protonation constants reported in Figure 3a.

$$k_{2nd} = k_{hydration} = \frac{[H^+]^2}{[H^+]^2 + K_a[H^+] + K_aK_{A/A^-}}k_h + \frac{1}{(1+K_t)}k_{-h}[H^+] + k_{OH}[OH^-] \quad (27)$$

When the hydration and OH^- nucleophilic addition rate constants are compared with those obtained in the absence of caffeine, $k_h = 0.12\ s^{-1}$, $k_{-h} = 35\ M^{-1}s^{-1}$, and $k_{OH} = 0.09\ M^{-1}s^{-1}$, and it can be concluded that the stabilization by intermolecular copigmentation decreases the rate constant k_h and increases k_{-h}, an effect already observed in intermolecular copigmentation of acylated anthocyanins.[19] The OH^- nucleophilic addition is also significantly reduced by the intermolecular copigmentation. Figure 4b shows the relative energy levels of the quinoidal base and hemiketal in the presence and absence of the copigment, calculated as reported in the literature.[14] The copigmentation stabilizes the quinoidal base and destabilizes the hemiketal. Clearly, it is a process to increase the color given by the quinoidal base, as can be visualized when comparing Figure 3c,d.

2.2. Irreversible Processes. The rate constants of the irreversible processes of malvidin-3-*O*-glucoside in the presence of caffeine 0.05 M were calculated and are represented in Figure 5a. Fitting was achieved by means of eq 28, where χ represents the mole fraction distribution of the quinoidal bases calculated in Figure 3b and $k_{irr.}$ the respective rate constants (degradation constants) with $k_{irr.(A)} = 2.5 \times 10^{-6}\ s^{-1}$, $k_{irr.(A-)} = 5.5 \times 10^{-6}\ s^{-1}$, and $k_{irr.(A2-)} = 6 \times 10^{-7}\ s^{-1}$

$$k_{irreversible} = \chi_A k_{irr.(A)} + \chi_{A^-}k_{irr.(A^-)} + \chi_{A^{2-}}k_{irr.(A^{2-})} \quad (28)$$

In the basic medium, the fitting was performed considering a similar process, given by eq 29, involving most probably Ct^{2-} and Ct^{3-} with pK = 11.3, $k_{irr.(Ct2-)} = 7 \times 10^{-7}\ s^{-1}$, and $k_{irr.(Ct3-)} = 3 \times 10^{-6}\ s^{-1}$, but there is a huge uncertainty in these values.

$$k_{irreversible} = \chi_{Ct^{2-}}k_{irr.(Ct^{2-})} + \chi_{Ct^{3-}}k_{irr.(Ct^{3-})} \quad (29)$$

In Figure 5b, the hydration and OH^- nucleophilic addition rates are represented together with the rates of the irreversible processes in the absence and presence of caffeine 0.05 M. Some conclusions can be taken from this figure. The hydration in the presence of the copigment is shifted to higher pH values. Representing the contributions for the hydration reaction rate of the term dependent on k_h (direct) and the term depending

https://doi.org/10.1021/acsomega.2c02571
ACS Omega 2022, 7, 25502−25509

on k_{-h} (reverse) in eq 27, as shown in Figure 5c, it can be concluded that there is an inversion. The hydration rate in the presence of the copigment is shifted to higher pH values, in comparison with the situation in the absence of the copigment, only for pH > 6.5. At these pH values, the influence of the constant k_{-h} is higher. The shift to higher pH values of the hydration curve in the presence of the copigment is explained by considering that the k_{-h} increases from 35 to 150 $M^{-1}s^{-1}$ in the presence of the copigment.

The OH^- nucleophilic addition is shifted to higher pH values, meaning that a higher OH^- concentration is necessary for hydroxylation to occur toward the equilibrium. The degradation rates of the *trans*-chalcones are also significantly decreased in the presence of the copigment caffeine.

2.3. Copigmentation at pH = 8.4. In the pH range where degradation is the controlling step, the rate of the anionic quinoidal basis disappearance is slow enough to allow for the determination of the copigmentation constant, as shown in Figure 6. Caffeine addition to a malvidin-3-*O*-glucoside solution 8.4×10^{-6} M at pH = 8.4 gives rise to a red shift and a hyperchromic effect, reinforcing the blue hue. Representation of the absorbance at 640 nm as a function of the caffeine concentration can be fitted for a 1:1 copigmentation with an association constant of 1.5×10^3 M^{-1} (estimated 5% error). For the caffeine concentration of 0.05 M, 99% of the malvidin-3-*O*-glucoside is involved in the copigmentation process. Despite the fact that degradation is significantly reduced in these conditions, it is still not enough for applications requiring relatively long storage times.

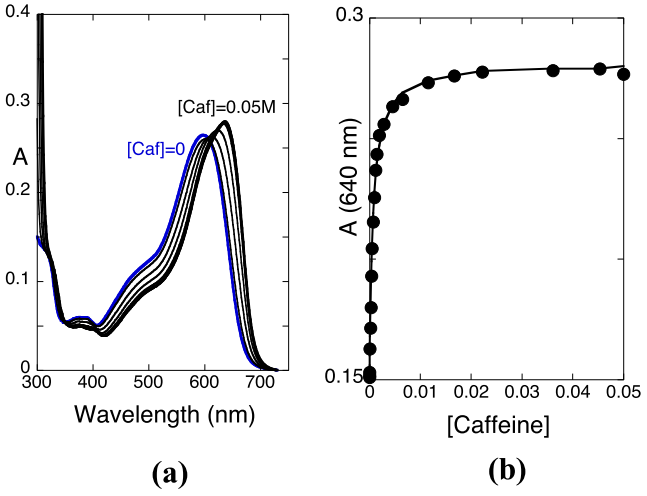

Figure 6. (a) Spectral variations upon the addition of caffeine (pH = 8.4) to a malvidin-3-*O*-glucoside solution at the same pH and (b) variation of the absorbance at 640 nm vs caffeine concentration. Fitting was achieved for a 1:1 copigmentation with an association constant of 1.5×10^3 M^{-1} (estimated 5% error).

3. EXPERIMENTAL SECTION

Malvidin-3-*O*-glucoside was purchased from Extrasynthese, and caffeine was obtained from Alfa Aesar Company Ltd. The Teorell and Stenhagen universal buffer[29] was prepared by dissolving 2.25 mL of phosphoric acid 85% (w/w), 7.00 g of monohydrated citric acid, 3.54 g of boric acid, and 343 mL of a 1 M NaOH solution in Millipore water until a volume of 1 L.

For the calculation of pK_a, pK'_a, and the pKs of the ionized forms, direct pH jumps were carried out by mixing the flavylium stock solution (1×10^{-4} M at pH = 1), NaOH to neutralize the amount of HCl added, buffer at the desired pH (with and without caffeine), and water (or caffeine 0.1 M in water). Reverse pH jumps were performed by adding enough HCl (with or without caffeine) to equilibrated or pseudo-equilibrated solutions to reach pH = 1. pH was recorded on a Radiometer Copenhagen PHM240 pH/ion meter (Brønshøj, Denmark).

UV−vis spectra were recorded on a Varian-Cary 100 Bio or 5000 spectrophotometer (Palo Alto, CA, USA). The reverse pH jumps from the pseudo-equilibrium were observed on an SX20 (Applied Photophysics; Surrey, UK) spectrometer equipped with a PDA.1/UV photodiode array detector. A filter of 385 nm was used to prevent the photochemical reactions that could take place from Cc or B.

4. CONCLUSIONS

Intermolecular copigmentation of malvidin-3-*O*-glucoside with caffeine affects both reversible and irreversible processes. It destabilizes hemiketal and stabilizes the colored quinoidal base. In the presence of the copigment, there is still a pH range where degradation of quinoidal bases is the faster process. Intermolecular copigmentation with caffeine is able to decrease the malvidin-3-*O*-glucoside degradation rate by a few folds. While this effect is not enough for applications requiring a relatively long storage time, it constitutes a basic knowledge to find a possible strategy to stabilize the color at neutral to slightly basic pH values. In this pH region, the kinetics of both hydration and OH^- nucleophilic addition are very slow. Protection of the quinoidal bases in this pH region could be a way to increase the lifetime of the blue color given by anthocyanins. Studies using cinnamic acids as copigments and degradation of acylated anthocyanins are in progress.

AUTHOR INFORMATION

Corresponding Author

Fernando Pina − *LAQV—REQUIMTE, Departamento de Química, Faculdade de Ciências e Tecnologia, Universidade Nova de Lisboa, Caparica 2829-516, Portugal;* orcid.org/0000-0001-8529-6848; Email: fp@fct.unl.pt

Authors

Ambrósio Camuenho − *LAQV—REQUIMTE, Departamento de Química, Faculdade de Ciências e Tecnologia, Universidade Nova de Lisboa, Caparica 2829-516, Portugal*

André Seco − *LAQV—REQUIMTE, Departamento de Química, Faculdade de Ciências e Tecnologia, Universidade Nova de Lisboa, Caparica 2829-516, Portugal;* orcid.org/0000-0003-0958-9651

A. Jorge Parola − *LAQV—REQUIMTE, Departamento de Química, Faculdade de Ciências e Tecnologia, Universidade Nova de Lisboa, Caparica 2829-516, Portugal;* orcid.org/0000-0002-1333-9076

Nuno Basílio − *LAQV—REQUIMTE, Departamento de Química, Faculdade de Ciências e Tecnologia, Universidade Nova de Lisboa, Caparica 2829-516, Portugal;* orcid.org/0000-0002-0121-3695

Complete contact information is available at: https://pubs.acs.org/10.1021/acsomega.2c02571

https://doi.org/10.1021/acsomega.2c02571
ACS Omega 2022, 7, 25502−25509

Author Contributions

This manuscript was written through contributions of all authors. All authors have given approval to the final version of the manuscript.

Notes

The authors declare no competing financial interest.

■ ACKNOWLEDGMENTS

This work was supported by the Associate Laboratory for Green Chemistry—LAQV which is financed by national funds from FCT/MCTES (UIDB/50006/2020 and UIDP/50006/2020). N.B. would like to thank Fundação para a Ciência e Tecnologia (FCT) for contracts CEECIND/00466/2017. A.S. and A.C. acknowledge their doctoral grants from FCT: 2020.07313.BD and Fundação Calouste Gulbenkian, grant no 219201.

■ REFERENCES

(1) Andersen, O. M.; Markham, K. R. *Flavonoids: Chemistry, Biochemistry, and Applications*; CRC Press: Boca Raton, FL, 2006.
(2) Harborne, J. B.; Williams, C. A. Advances in Flavonoid Research since 1992. *Phytochemistry* **2000**, *55*, 481−504.
(3) Hoballah, M. E.; Gubitz, T.; Stuurman, J.; Broger, L.; Barone, M.; Mandel, T.; Dell'Olivo, A.; Arnold, M.; Kuhlemeier, C. Single Gene-Mediated Shift in Pollinator Attraction in Petunia. *Plant Cell* **2007**, *19*, 779−790.
(4) Ahmed, N. U.; Park, J.-I.; Jung, H.-J.; Yang, T.-J.; Hur, Y.; Nou, I.-S. Characterization of Dihydroflavonol 4-Reductase (Dfr) Genes and Their Association with Cold and Freezing Stress in Brassica Rapa. *Gene* **2014**, *550*, 46−55.
(5) Chalker-Scott, L. Environmental Significance of Anthocyanins in Plant Stress Responses. *Photochem. Photobiol.* **1999**, *70*, 1−9.
(6) Guo, J.; Wang, M.-H. Ultraviolet a-Specific Induction of Anthocyanin Biosynthesis and Pal Expression in Tomato (Solanum Lycopersicum L.). *Plant Growth Regul.* **2010**, *62*, 1−8.
(7) Zhu, H.; Zhang, T. J.; Zheng, J.; Huang, X. D.; Yu, Z. C.; Peng, C. L.; Chow, W. S. Anthocyanins Function as a Light Attenuator to Compensate for Insufficient Photoprotection Mediated by Non-photochemical Quenching in Young Leaves of Acmena Acuminatissima in Winter. *Photosynthetica* **2018**, *56*, 445−454.
(8) Fernandes, I.; Pérez-Gregorio, R.; Soares, S.; Mateus, N.; De Freitas, V. Wine Flavonoids in Health and Disease Prevention. *Molecules* **2017**, *22*, 292.
(9) Quideau, S.; Deffieux, D.; Douat-Casassus, C.; Pouységu, L. Plant Polyphenols: Chemical Properties, Biological Activities, and Synthesis. *Angew. Chem., Int. Ed.* **2011**, *50*, 586−621.
(10) Bars-Cortina, D.; Sakhawat, A.; Piñol-Felis, C.; Motilva, M.-J. Chemopreventive Effects of Anthocyanins on Colorectal and Breast Cancer: A Review. *Semin. Cancer Biol.* **2022**, *81*, 241.
(11) Ma, Y.; Ding, S.; Fei, Y.; Liu, G.; Jang, H.; Fang, J. Antimicrobial Activity of Anthocyanins and Catechins against Foodborne Pathogens Escherichia Coli and Salmonella. *Food Control* **2019**, *106*, 106712.
(12) Oliveira, H.; Fernandes, I.; de Freitas, V.; Mateus, N. Ageing Impact on the Antioxidant and Antiproliferative Properties of Port Wines. *Food Res. Int.* **2015**, *67*, 199−205.
(13) Enaru, B.; Dreţcanu, G.; Pop, T. D.; Stănilă, A.; Diaconeasa, Z. Anthocyanins: Factors Affecting Their Stability and Degradation. *Antioxidants* **2021**, *10*, 10.
(14) Cruz, L.; Basílio, N.; Mateus, N.; de Freitas, V.; Pina, F. Natural and Synthetic Flavylium-Based Dyes: The Chemistry Behind the Color. *Chem. Rev.* **2022**, *122*, 1416−1481.
(15) Malien-Aubert, C.; Dangles, O.; Amiot, M. J. Influence of Procyanidins on the Color Stability of Malvidin-3-O-glucoside Solutions. *J. Agric. Food Chem.* **2002**, *50*, 3299−3305.
(16) Fenger, J.-A.; Moloney, M.; Robbins, R. J.; Collins, T. M.; Dangles, O. The Influence of Acylation, Metal Binding and Natural Antioxidants on the Thermal Stability of Red Cabbage Anthocyanins in Neutral Solution. *Food Funct.* **2019**, *10*, 6740−6751.
(17) Brouillard, R.; Dubois, J.-E. Mechanism of Structural Transformations of Anthocyanins in Acidic Media. *J. Am. Chem. Soc.* **1977**, *99*, 1359−1364.
(18) Brouillard, R.; Delaporte, B.; Dubois, J. E. Chemistry of Anthocyanins Pigments.3. Relaxation Amplitudes in Ph-Jump Experiments. *J. Am. Chem. Soc.* **1978**, *100*, 6202−6205.
(19) Sousa, D.; Basílio, N.; Oliveira, J.; de Freitas, V.; Pina, F. A New Insight into the Degradation of Anthocyanins: Reversible Versus the Irreversible Chemical Processes. *J. Agric. Food Chem.* **2022**, *70*, 656−668.
(20) McClelland, R. A.; Gedge, S. Hydration of the Flavylium Ion. *J. Am. Chem. Soc.* **1980**, *102*, 5838−5848.
(21) Mendoza, J.; Basílio, N.; de Freitas, V.; Pina, F. New Procedure to Calculate All Equilibrium Constants in Flavylium Compounds: Application to the Copigmentation of Anthocyanins. *ACS Omega* **2019**, *4*, 12058−12070.
(22) McClelland, R. A.; McGall, G. H. Hydration of the Flvylium Ion.2. The 4′-Hydroxyflavylium Ion. *J. Org. Chem.* **1982**, *47*, 3730−3736.
(23) Escribano-Bailon, M. T.; Santos-Buelga, C. Anthocyanin Copigmentation—Evaluation, Mechanisms and Implications for the Colour of Red Wines. *Curr. Org. Chem.* **2012**, *16*, 715−723.
(24) Eiro, M. J.; Heinonen, M. Anthocyanin Color Behavior and Stability During Storage: Effect of Intermolecular Copigmentation. *J. Agric. Food Chem.* **2002**, *50*, 7461−7466.
(25) Trouillas, P.; Sancho-García, J. C.; De Freitas, V.; Gierschner, J.; Otyepka, M.; Dangles, O. Stabilizing and Modulating Color by Copigmentation: Insights from Theory and Experiment. *Chem. Rev.* **2016**, *116*, 4937−4982.
(26) Oliveira, J.; Azevedo, J.; Seco, A.; Mendoza, J.; Basílio, N.; de Freitas, V.; Pina, F. Copigmentation of Anthocyanins with Copigments Possessing an Acid-Base Equilibrium in Moderately Acidic Solutions. *Dyes Pigm.* **2021**, *193*, 109438.
(27) Oliveira, J.; Azevedo, J.; Teixeira, N.; Araújo, P.; de Freitas, V.; Basílio, N.; Pina, F. On the Limits of Anthocyanins Co-Pigmentation Models and Respective Equations. *J. Agric. Food Chem.* **2021**, *69*, 1359−1367.
(28) Araújo, P.; Basílio, N.; Fernandes, A.; Mateus, N.; de Freitas, V.; Pina, F.; Oliveira, J. Impact of Lignosulfonates on the Thermodynamic and Kinetic Parameters of Malvidin-3-O-Glucoside in Aqueous Solutions. *J. Agric. Food Chem.* **2018**, *66*, 6382−6387.
(29) Küster, F. W.; Thiel, A. *Tabelle Per Le Analisi Chimiche E Chimico- Fisiche*, 12th ed.: Milano, Italy; Hoepli, 1982; pp 157−160.

https://doi.org/10.1021/acsomega.2c02571
ACS Omega 2022, 7, 25502−25509